ORIGINAL RESEARCH ARTICLE

Microplankton size structure induced by a warm-core eddy in the western Bay of Bengal: Role of *Trichodesmium* abundance

Karnan Chinnadurai[a,b], Jyothibabu Retnamma[a,*], Arunpandi Nagarathinam[a], Pandiyarajan Rethinam Subramanian[a], Parthasarathi Singaram[a], Santhikrishnan Shoba[a]

[a] *CSIR — National Institute of Oceanography, Regional Centre, Kochi, India*
[b] *CSIR — National Institute of Oceanography, Dona Paula, Goa, India*

Abstract Mesoscale warm-core eddies are common in the Bay of Bengal (BoB), and this study in the western BoB during Pre-Southwest Monsoon (April 2015) presents how a prolonged warm-core core eddy could modify the microplankton biomass and size structure. To investigate this, field sampling and laboratory analyses were augmented with satellite data sets of sea surface temperature (SST), winds, mean sea level anomaly (MSLA), geostrophic currents and chlorophyll-*a*. High SST with positive MSLA ($\geq$ 20 cm) and a clockwise circulation, represented the occurrence of a large warm-core eddy in the western BoB. Time series data evidenced that it was originated in the mid of March and persistent there till early June, which in turn caused a decrease in the surface nutrients and chlorophyll-*a*. The abundance and biomass of microplankton were negligible in the warm-core eddy region. FlowCAM data showed a significant decrease in the autotrophic microplankton parameters in the warm-core eddy (av. 13 $\pm$ 9 ind. L^{-1} and 0.1 $\pm$ 0.04 μgC L^{-1}, respectively) as compared to the surrounding locations (av. 227 $\pm$ 143 ind. L^{-1} and 0.8 $\pm$ 0.5 μgC L^{-1}, respectively). Low nutrients level in the warm core eddy region favoured high abundance of needle-shaped phytoplankton cells dominated by *Trichodesmium*

* Corresponding author at: CSIR — National Institute of Oceanography, Regional Centre, Kochi, India. Telephone: +91 484 2390814; Fax: +91 484 2390618.
 E-mail address: rjyothibabu@nio.org (J. Retnamma).
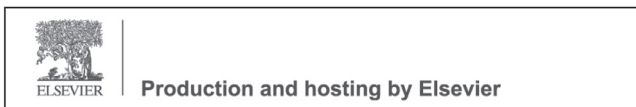
cells. As a result, the size of micro-autotrophs in the warm-core eddy was larger (av. 91,760 $\pm$ 12,902 μm^3 ind.$^{-1}$) than its outside (av. 50,115 $\pm$ 21,578 μm^3 ind.$^{-1}$). This is a deviation from our belief that the oligotrophy decreases the phytoplankton size. We showed here that the above understanding might not be infallible in warm-core eddies in the northern Indian Ocean due to its inducing effect on the *Trichodesmium* abundance.

1. Introduction

The analysis of community composition, size and biomass of plankton are important for understanding the biological/fishery characteristics of an aquatic ecosystem (Chassot et al., 2010; Harrison et al., 2015). Generally, nutrient-rich water bodies are much more productive and contain a high abundance of large autotrophs, whereas low-nutrient (oligotrophic) environments are less so, facilitating the dominance of small phytoplankton (Garrison et al., 2000; Landry et al., 1998; Wong et al., 2016). The microplankton (20—200 μm) consists of both autotrophs and heterotrophs which are sensitive to hydrographical changes. The micro-autotrophs are larger phytoplankton, which is significant in producing and transferring a large amount of organic carbon to higher trophic levels in the food chain. The micro-heterotrophs are the micro-zooplankton, the key components of the microbial food web, which transfer the biomass of smaller auto and heterotrophic plankton (pico- and nano-sized) to higher trophic levels (mesozooplankton and above) (Azam et al., 1983). The Bay of Bengal (BoB), situated in the eastern part of the northern Indian Ocean, is significantly less productive than its western counterpart, the Arabian Sea, despite receiving a large quantity of freshwater (1.6 $\times$ 10^{12} m^3 yr^{-1}) and suspended sediments (1.4 $\times$ 10^9 tonnes yr^{-1}) from several major rivers of India, Bangladesh and Myanmar (Madhupratap et al., 2003; Subramanian, 1993). The biological productivity in the BoB is limited by a combination of multiple hydrographical parameters, pivotally by nutrients, light, temperature and salinity (Gauns et al., 2005; Gomes et al., 2000; Jyothibabu et al., 2018; Prasanna Kumar et al., 2010; Sarma et al., 2020). The BoB is getting nutrients through riverine, wind-induced mixing of the surface ocean, eddy pumping, coastal upwelling, ocean currents and aeolian processes (Gomes et al., 2000; Mukhobadhyay et al., 2006; Patra et al., 2007; Prasanna Kumar et al., 2004; Vinayachandran et al., 2004). The shallow vertical mixing in the BoB due to density and temperature-induced stratification and weaker winds over the region significantly control the vertical nutrient flux to the euphotic column and thus, they control biological productivity (Prasanna Kumar et al., 2002; Shenoi et al., 2002).

The seasonally reversing monsoonal winds and currents have a significant role in regulating the biogeochemical cycles in the BoB. The well-documented seasonally-reversing coastal currents system along the east coast of India is known as East India Coastal Current (EICC).

The EICC flows pole-ward during the February—September period (intense in March—May) and reverses equator-ward during October—January (intense in November) (Patnaik et al., 2014; Shankar et al., 1996; Shetye et al., 1991; Vinayachandran et al., 2009). Along with these basin-scale features, mesoscale features (10s to 100s of km) also influence plankton productivity and material cycling through the biological pump (Chelton et al., 2011; Jyothibabu et al., 2015, 2017; Mahadevan et al., 2012; Prasanna Kumar et al., 2002).

The mesoscale eddies are formed by the meandering/reverse currents from the turbulent flow of a water current due to baroclinic instability and propagate away from the mainstream (Durand et al., 2009; Mahadevan et al., 2014). The eddy, which pinched off from the main current may retain the hydrographic properties, and even carry organisms of the original water mass for a long period transporting them at a long distance (Jagadeesan et al., 2019). The cyclonic and anticyclonic eddies exist plentifully in the BoB (Chen et al., 2012; Dandapath and Chakraborty, 2016) and most of them are formed in the eastern/north-eastern BoB and propagate to western/south-western BoB (Cheng et al., 2018). It has been observed that cyclonic/cold-core eddies pump nutrients to the surface of euphotic column, thereby enhancing new production (Jyothibabu et al., 2008; McGillicuddy et al., 1998; Prasanna Kumar et al., 2004). However, it was also observed that the effect of cold-core eddy in the BoB is restricted only to the subsurface (below 20 m), due to capping of low saline water mass at the surface (Gauns et al., 2005; Jyothibabu et al., 2008; Prasanna Kumar et al., 2004). On the other hand, anticyclonic/warm-core eddies in the BoB converge and sink the nutrient-depleted surface waters towards the subsurface, thereby intensifying the oligotrophy of the upper euphotic column (Chelton et al., 2011; Jyothibabu et al., 2017; McGillicuddy et al., 2003; Sarma et al., 2020).

It is generally believed that among different phytoplankton size groups, micro-phytoplankton dominate in chlorophyll/biomass production in nutrient-rich coastal/shelf waters and mesoscale eddy-infested (cold) regions (Jyothibabu et al., 2015; Karnan et al., 2017; Sarma et al., 2020; Yentsch and Phinney, 1989). A recent study conducted by Sarma et al. (2020) in the central and western BoB presented the size-fractionated primary productivity. However, there is a general lack of quantitative data on the plankton community size distribution associated with different ocean
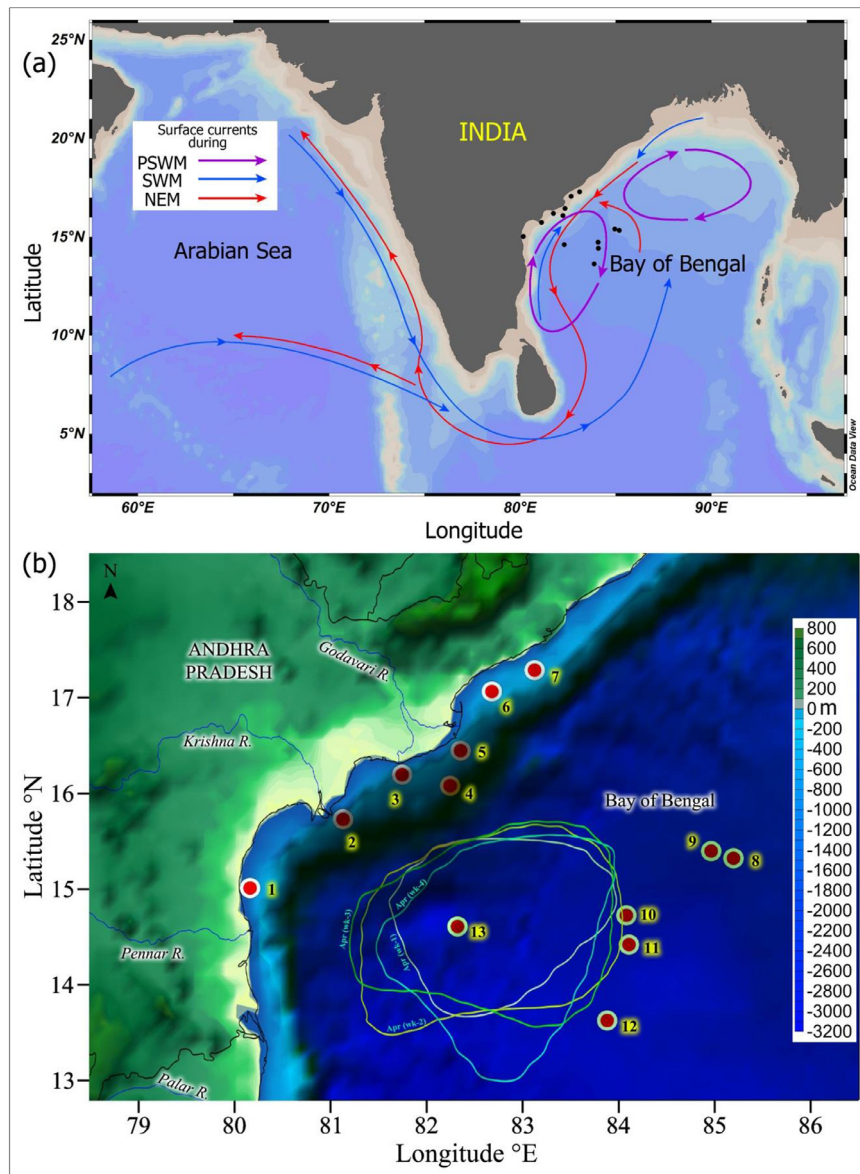
Figure 1 (a) Sampling locations in the western Bay of Bengal and the seasonal circulation patterns as marked in different coloured arrows (violet: Pre-Southwest Monsoon; blue: Southwest Monsoon and red: Northeast Monsoon) over the northern Indian Ocean. (b) Sampling locations 1—7 in the shelf waters and locations 8—13 in the oceanic waters. Panel (b) shows strong warm-core eddy prevailed in the area with a certain spatial shift over time as shown in the multicoloured contours (MSL + 25 cm) for each week.

processes (Harrison et al., 2015; Karnan et al., 2017). Hence, in this study, focused attempts have been made to understand the spatial variation in the micro-plankton size structure in the western BoB infested with a strong mesoscale warm-core eddy during the Pre-Southwest Monsoon period. It is hypothesized here that as the oligotrophic warm-core eddy enhances the *Trichodesmium* abundance, it could facilitate an exceptional microplankton size structure compared to the rest of the region. The major objectives in this study include (a) the role of persistent warm-core mesoscale eddies in defining the micro-plankton size structure, (b) spatial variations in the micro-plankton size and shape, and (c) role of warm-core eddies in controlling the chlorophyll-*a* biomass in the western BoB.

2. Material and methods

2.1. Study area

As mentioned above, the Bay of Bengal (BoB) is a low productive region of the northern Indian Ocean, even though the region receives an enormous quantity of freshwater from several major rivers (Subramanian, 1993). The low salinity and less dense surface water create density stratification, which inhibits surface layer mixing and leads to nutrient-depleted waters in the upper euphotic column (Gauns et al., 2005). The study region in the western BoB is characterized by seasonally reversing EICC (Figure 1a). The role of coastal currents is pivotal in the dynamics of water

mass and the formation of mesoscale eddies in the present study area, causing changes in the distribution of nutrients and biological communities.

2.2. Sampling methods

Field sampling was conducted during April 2015 (4—20th) in the central-western BoB and water samples were collected onboard r/v *Sindhu Sadhana* from 13 locations (Figure 1b). Sampling locations were distributed from ~60 m depth up to ~3,250 m depth. The hydrography of the water column was assessed by taking measurements of physicochemical and biological parameters. Temperature, salinity and chlorophyll-*a* were measured using respective sensors attached with a CTD rosette (Seabird Electronics, USA). Usually, the warm-core eddies have deep mixed layer depths (MLD) and here, we collected representative samples from 5 m depth (hereafter surface samples) using a Niskin sampler from all locations. The major nutrients such as nitrate (NO_3), phosphate (PO_4) and silicate (SiO_4) were analysed following the standard protocols (Grasshoff et al., 1983). 5 L of water collected from each Niskin sampler was pre-filtered with a 300 μm mesh and concentrated by siphoning with a 20 μm mesh to 0.5 L as presented in Karnan et al. (2017). The concentrated water samples were preserved and fixed with 3% Lugol's iodine solution and stored in dark polythene bottles. In the laboratory, samples were analysed through a FlowCAM and light microscopy.

2.3. Satellite data sets

A variety of satellite-derived data have been used in this study. The sea surface temperature (SST; MODIS AQUA), wind (ASCAT), mean sea level anomaly (MSLA; AVISO), geostrophic currents (AVISO) and chlorophyll-*a* (MODIS AQUA) were the major satellite datasets downloaded from online data access servers for the respective sampling region (oceanwatch.pifsc.noaa.gov, aviso.altimetry.fr, and aoml.noaa.gov). The weekly averages of each dataset were created with integrative plots to understand the combined effect of these processes during the sampling period. Also, monthly variations of these parameters were presented (2015) to understand their distribution in the sampling domain. Standard software tools were used to analyze satellite data sets (PyFerret 7.4) and plotting (ODV 5.3 and Grapher 8.7).

2.4. Eddy detection

We used a combination of auto- (contour generation) and an expert detection (manual checking) method to distinguish mesoscale eddies in the western BoB (Chaigneau et al., 2008; Li et al., 2015). The weekly means of satellite altimetry products (MSLA, zonal and meridional components of geostrophic currents) were retrieved from AVISO (Archiving, Validation and Interpretation of Satellite Oceanographic data) live access server. The data sets were processed together in the PyFerret software tool (v7.4) to generate MSLA maps with 1 cm contour interval and overlaid with geostrophic currents. The output images were visually analyzed to detect eddies by checking the presence of multiple (> 3) closed contours of MSLA and a circulation pattern

of geostrophic currents. Vinayachandran et al. (2009) preferred 10 cm MSL anomaly as a criterion to detect eddies, and we used 20 cm MSL anomaly as a criterion (< -20 cm as cold and > 20 cm as warm-core) to distinguish stronger mesoscale eddies. To show the impact of the warm-core eddy on SST and chlorophyll-*a*, we have overlaid 25 cm MSLA contours on weekly mean images. The time series of MSLA data sets were plotted on longitude-time axes and latitude-time axes to understand the origin and propagation of eddies. The MSLA data of the longitude-time plot was centred at 14.9°N and the latitude-time plot was centred at 82.9°E, where we noticed the highest MSLA of the warm-core eddy.

2.5. Laboratory analysis of plankton samples

Water samples were analysed through a portable FlowCAM and images of particles present in samples were captured (Karnan et al., 2017). The preserved plankton samples were diluted with filtered saline water to remove the pungency of Lugol's iodine and concentrated to 20 mL. In FlowCAM, the hardware components such as 300 μm flow cell with 100% field of view (FOV) with a combination of 4X objective lens were used and images were captured in auto image mode. In this mode, all particles were imaged at regular intervals and each sample was manually classified up to the genera level. Along with each image, its morphological properties such as length, width, diameter, aspect ratio and volume were exported. The carbon biomass of the individual plankton was estimated from its biovolume by applying the respective numerical conversion factors (Menden-Deuer and Lessard, 2000; Verity et al., 1992). The shape of plankton was assessed based on the aspect ratio (AR). The AR ranges between 0 to 1, in which low range (0—0.4) indicates cylindrical/needle shape and high range (0.6—1) indicates spheroid/sphere shape (Alvarez et al., 2012).

2.6. Statistical analyses

We used Pearson multiple correlation analysis to understand the relationship among the physicochemical and biological parameters using corrgram package in R-Studio (Friendly, 2002). The correlation matrix is presented as a shade with the line in the lower-left diagonal in which, red shade with downslope lines represent negative and blue shade with upslope lines represent the positive correlation. The correlation coefficients are presented in upper right diagonal with red (− values) and blue (+ values) colours.

3. Results

3.1. Sea Surface Temperature (SST)

The synoptic view of SST in the sampling region shows the occurrence of a large warm pool of water (Figure 2a). The overlaid MSLA contour (+25 cm) on the SST plot clearly shows the close association of the warm pool water with the warm-core eddy. Also, the strong EICC ($\geq$ 0.7 m/s) carries warm water along the east coast and around the eddy. The regional weekly mean SST ranged from av. 29.4 $\pm$ 0.2 to av. 29.8 $\pm$ 0.3°C. Overall, the northern part of the study
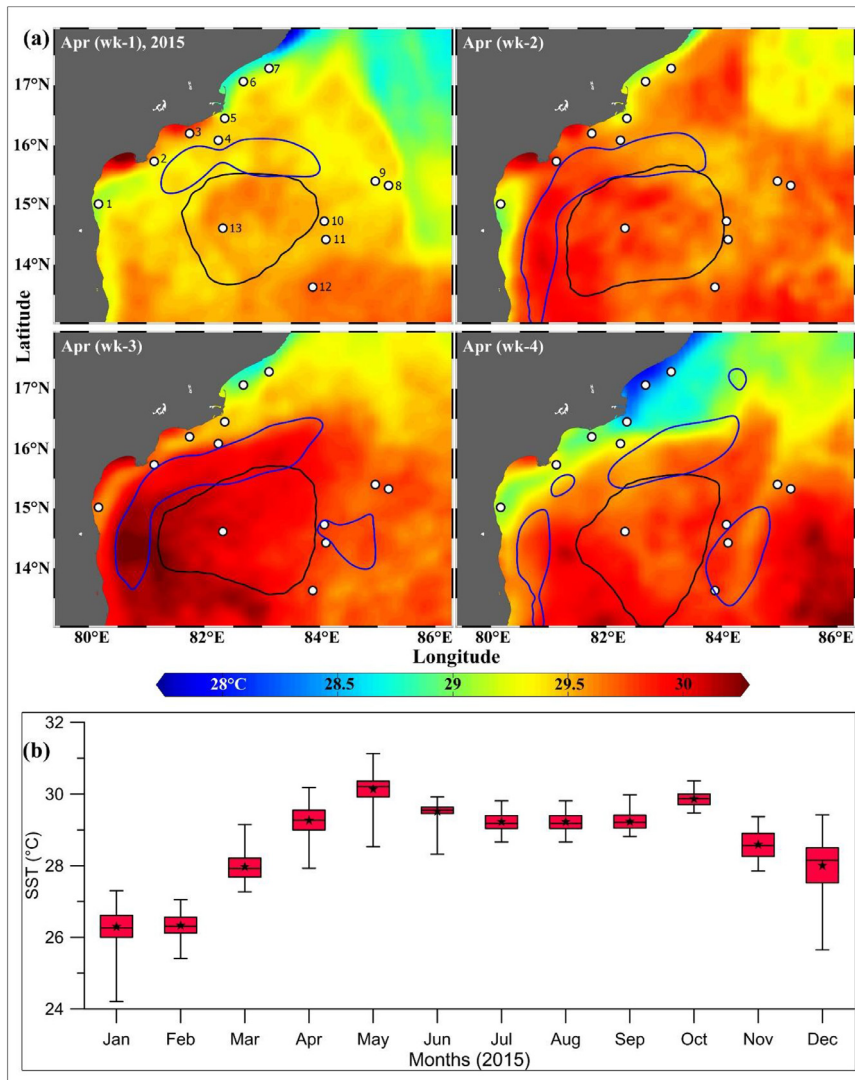
Figure 2   (a) Weekly distribution of sea surface temperature (SST) in the sampling region overlaid with contours of strong warm-core eddy (black line; MSL + 25 cm) and high geostrophic velocity (blue line; ≥ 0.7 m s^{-1}) in April 2015. In panel (b), the monthly distribution of SST in the sampling region is represented by box plot (error bars: lowest and highest values; box: 1st quartile, median and 2nd quartile), wherein the star marks represent the mean SST.

area was found to be cooler than the south. In specific, the presence of cooler water in the north-east coastal region shows the possibilities of cold-core eddy/coastal upwelling (Figure 2a). The SST showed a positive relationship with MSLA and size of autotrophs (r = 0.28, 0.37, respectively; Figure 10a). The monthly distribution of SST over sampling area showed warmer surface ocean throughout the year (2015; > 28°C), except during the late Northeast Monsoon period (January—February; av. 26.3°C). The peak SST was noticed during Pre-Southwest Monsoon, especially in May (av. 30.1 ± 0.3°C) followed by October (av. 29.9 ± 0.2°C; Figure 2b).
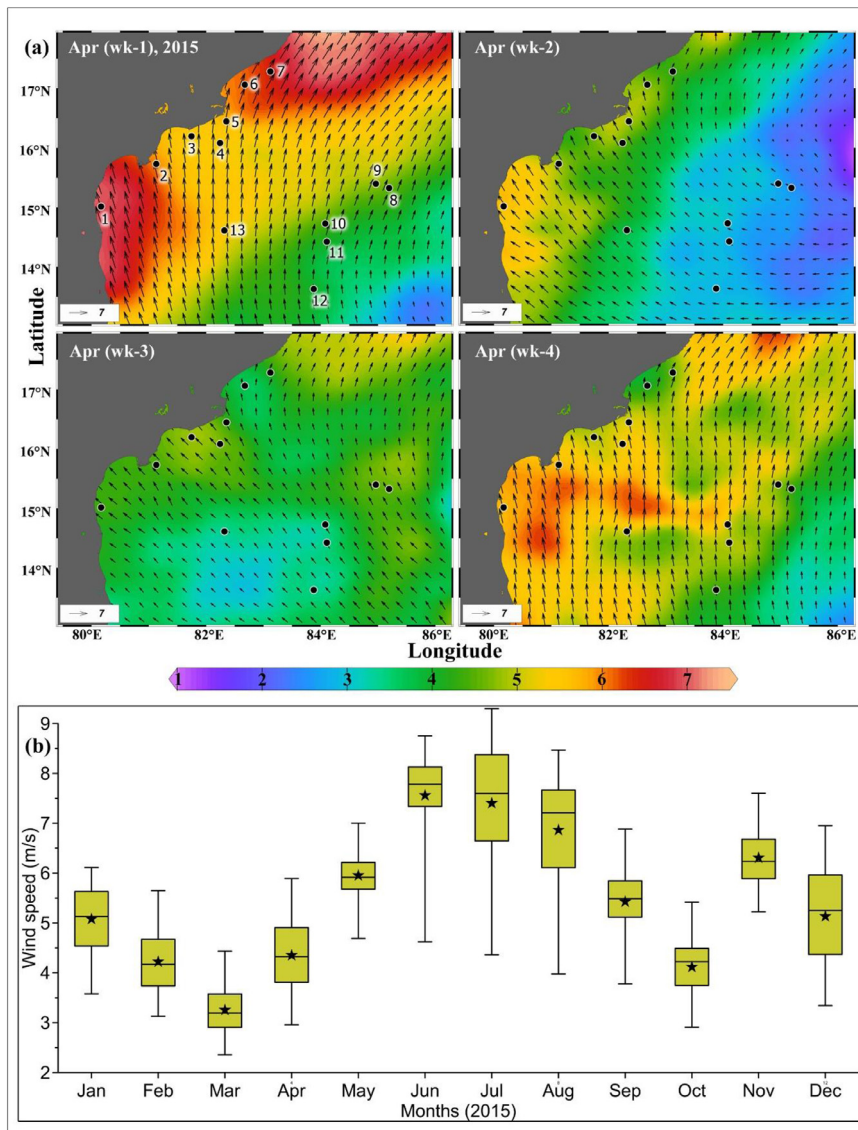
3.2. Wind velocity

The wind speed in the sampling region showed a decreasing trend from the first week (av. 5.9 ± 1.7 m s^{-1}) to the fourth week (av. 3 ± 1.6 m s^{-1}) in April 2015 (av. 4.4 ± 0.7 m s^{-1}).

The wind direction shifted from south-westerly to southerly and south-easterly during the sampling period (Figure 3a). The wind speed was comparatively stronger along/closer to the coastal region than offshore during most of the sampling period. The monthly mean wind speed over the sampling region for the year 2015 showed (Figure 3b) weakest during the inter monsoon months (March: av. 3.3 ± 0.5 m s^{-1} and October: av. 4.1 ± 0.5 m s^{-1}) and strongest during South-west Monsoon months (June—July: av. 7.5 ± 1 m s^{-1} and August: av. 6.9 ± 1 m s^{-1}). The annual mean wind speed was av. 5.5 ± 1.5 m s^{-1} in the sampling region.

3.3. MSLA and geostrophic currents

The weekly MSLA overlaid with corresponding geostrophic currents presented the northward-flowing EICC along the western boundary of the BoB with a velocity of 0.5—0.95 m s^{-1} (Figure 4a). The EICC is deflected eastward due to

Figure 3 (a) The weekly distribution of wind velocity over the sampling region in April 2015. In panel (b), the monthly distribution of wind velocity in the sampling region is represented in a box plot with the star mark representing the mean wind speed.

the topographic hindrance of the Indian sub-continent. The offshore-ward deflection and return current of mainstream created a clockwise circular motion of water mass with a velocity of > 0.5 m s^{-1}, which significantly converged the warmer surface water towards its core and caused a strong warm-core eddy circulation. The height of the eddy core was ranged from 34.7 cm to 38.6 cm, whereas the adjacent/coastal region has negative or near zero during the sampling period. The area of eddy calculated by applying 20 cm MSLA contour was ~93,580 km^2 and the diameter of the eddy was ~345 km. Also, two cold-core eddies (relatively smaller) were found during the sampling period, one along the northern coastline and another in the offshore. The MSLA is negatively correlated to nutrients and autotrophic abundance and biomass (Figure 10a). The monthly distribution of MSLA showed a significant dominance of positive mean sea level (2.1 ± 7.7 cm to 9.9 ± 10.7 cm) in the sampling domain, which indicates the presence/dominance of warm-core eddies throughout the year 2015 (Figure 4b). It

shows that a large area of the sampling domain was occupied by warm-core eddies during April—May and also, there were possibilities for the occurrence of cold-core eddies during September—November (Figure 4b). The longitude-time and latitude-time plots evidenced that the warm-core eddy was originated in the western BoB between 12°N—16°N and 81°E—85°E (Figure 5). The warm-core eddy was very prolonged, it originated in mid-March and was extinct in early-June. The strong EICC and its deflection during these periods could be the sole reason for the origin and strengthening of the warm-core eddy.

3.4. Salinity and nutrients

During the *in situ* sampling, surface salinity ranged from 33.1—34.4 (Figure 6a; Table 1). In contrast to the general view, coastal waters have slightly higher salinity (av. 33.9 ± 0.11) than the offshore waters (av. 33.3 ± 0.05), which evidences that the northward-flowing EICC carries high salinity
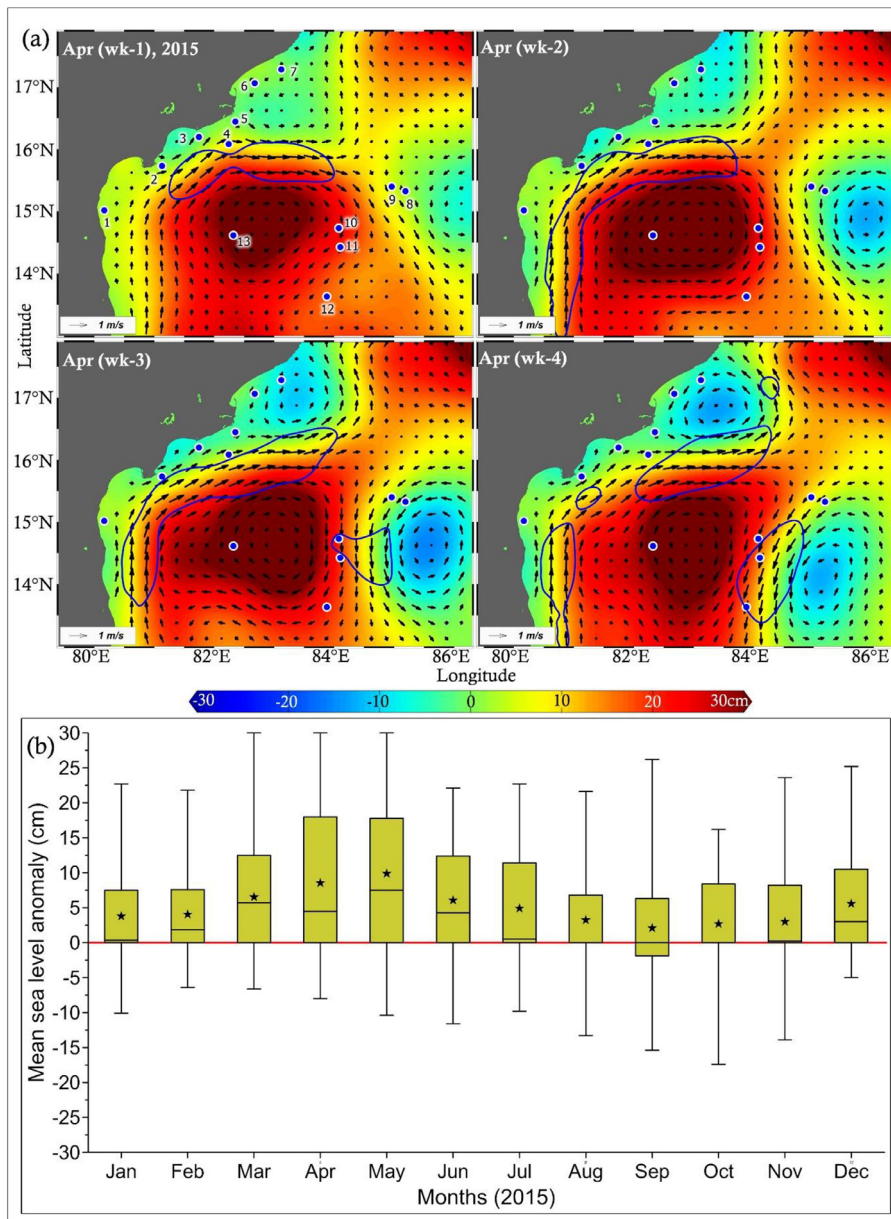
Figure 4 (a) The weekly time-series of mean sea level anomaly (MSLA) overlaid with geostrophic currents evidencing the existence of strong warm-core eddy over a month in the sampling region. The blue contour line indicates the swift geostrophic currents (velocity 0.7 m/s). Panel (b) shows the monthly distribution of MSLA in the sampling region represented as a box plot and the mean sea level in each month is indicated with a star mark. The MSLA values were truncated to ± 30 cm.

water from the southern part of the BoB. The concentration of major nutrients in the surface waters showed noticeable spatial differences (Figure 6b; Table 1). The concentration of nitrate (NO_3) was $< 1 \mu M L^{-1}$ at all locations; importantly, coastal/non-eddy locations had higher concentrations (av. $0.64 \pm 0.07 \mu M L^{-1}$) as compared to the offshore/warm-core eddy waters (av. $0.2 \pm 0.04 \mu M L^{-1}$). However, other nutrients such as silicate (SiO_4) and phosphate (PO_4) did not show much difference. Silicate in the non-eddy regions was slightly higher (av. $12.3 \pm 1.5 \mu M L^{-1}$) than the eddy region (av. $11.2 \pm 0.8 \mu M L^{-1}$). Similar was the case of PO_4, which was slightly higher in the non-eddy region (av. $0.23 \pm 0.03 \mu M L^{-1}$) than the eddy region (av. $0.2 \pm 0.03 \mu M L^{-1}$). The salinity and major nutrients were positively correlated

(Figure 10a). Overall nutrient distribution showed that the warm-core eddy had relatively poor nutrient levels.

3.5. Chlorophyll-*a*

Satellite-derived chlorophyll-*a* during April clearly showed high concentration along the coastal stretch and outside of the warm-core eddy boundary compared to the warm-core eddy region (Figure 7a; Table 1). Weekly contour lines of 25 cm positive MSLA (strong warm-core) were overlaid on the spatial image of chlorophyll-*a*, which encircled the lowest concentration of chlorophyll-*a*, evidencing the strong negative effect of the warm-core eddy. An extension of chlorophyll-*a* patches towards offshore (~16°N; > 0.15
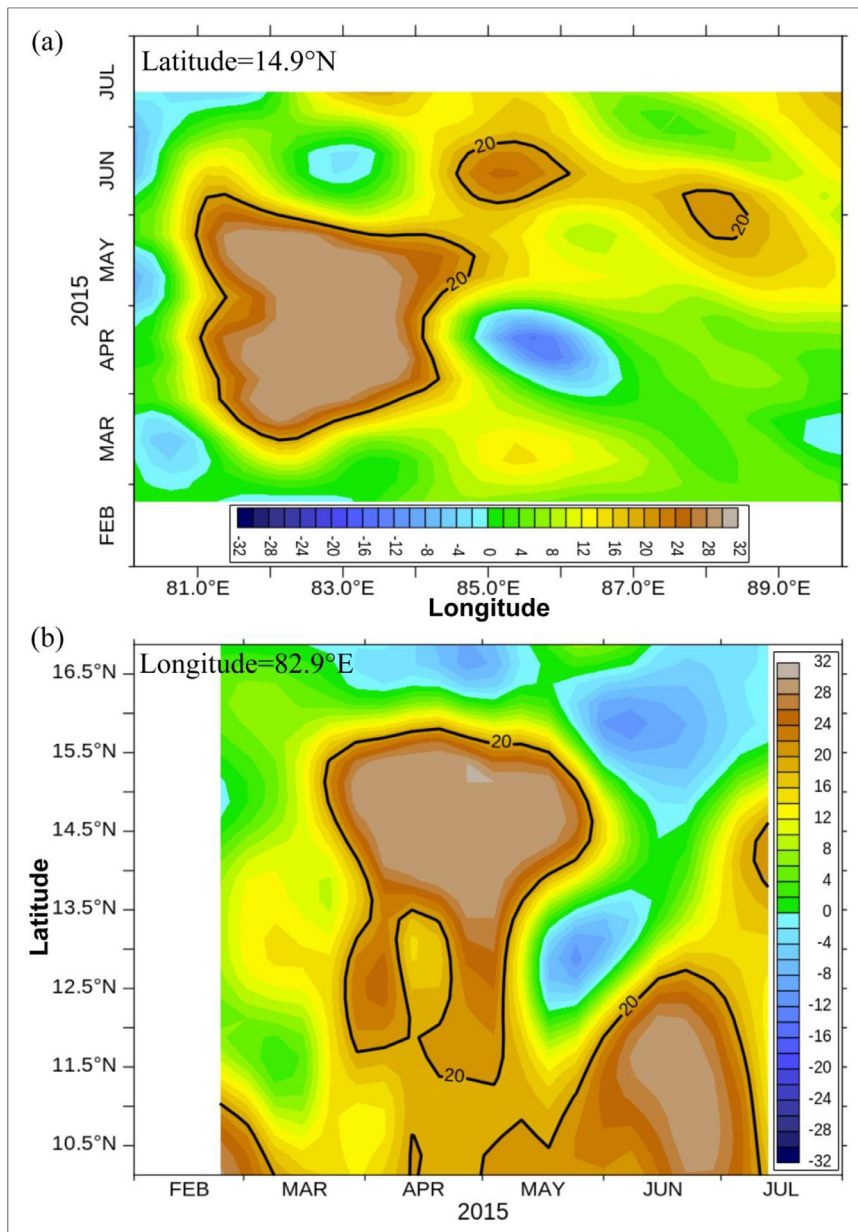
Figure 5 The warm-core eddy propagation represented by plotting MSLA on (a) longitude-time axes and (b) latitude-time axes. The positive MSLA (20 cm) contour evidenced the origin and extinction of warm-core eddy in the western BoB.

mg m^{-3}) indicates the effect of EICC which deflected over the curve-like topography of the sampling domain (around 16°N) of Indian sub-continent and could carry water from the continental shelf and a cold-core eddy (near-shore) in the north and fed the offshore region. Relatively high chlorophyll-*a* values in the offshore/east of warm-core eddy show the combined effect of shelf passed EICC and cold-core eddy (offshore). Chlorophyll-*a* was positively related to nutrients and autotrophic plankton parameters (abundance and biomass) but negative to SST and MSLA. The monthly mean chlorophyll-*a* in the sampling domain showed low concentration throughout the year and most of the area in the sampling domain was reflected in oligotrophy (Figure 7b). The lowest concentration (av. 0.27 mg m^{-3}) in a large surface area of the western BoB was found between

February and June and the remaining periods showed comparatively high values (av. 0.42 mg m^{-3}). The chlorophyll-*a* concentration in deep chlorophyll maxima layers in the offshore locations (8—13) reflected eddy impacts as the lowest concentration were detected closer to warm-core eddy, and relatively higher values were observed away from the warm-core eddy or near cold-core eddy (Supplementary Figure 1).

3.6. Autotrophic plankton composition, size and shape

The highest micro-phytoplankton abundance and biomass were found at location 1 (496 ind. L^{-1}; 0.7 μgC L^{-1}, respectively). The overall abundance and biomass of micro-
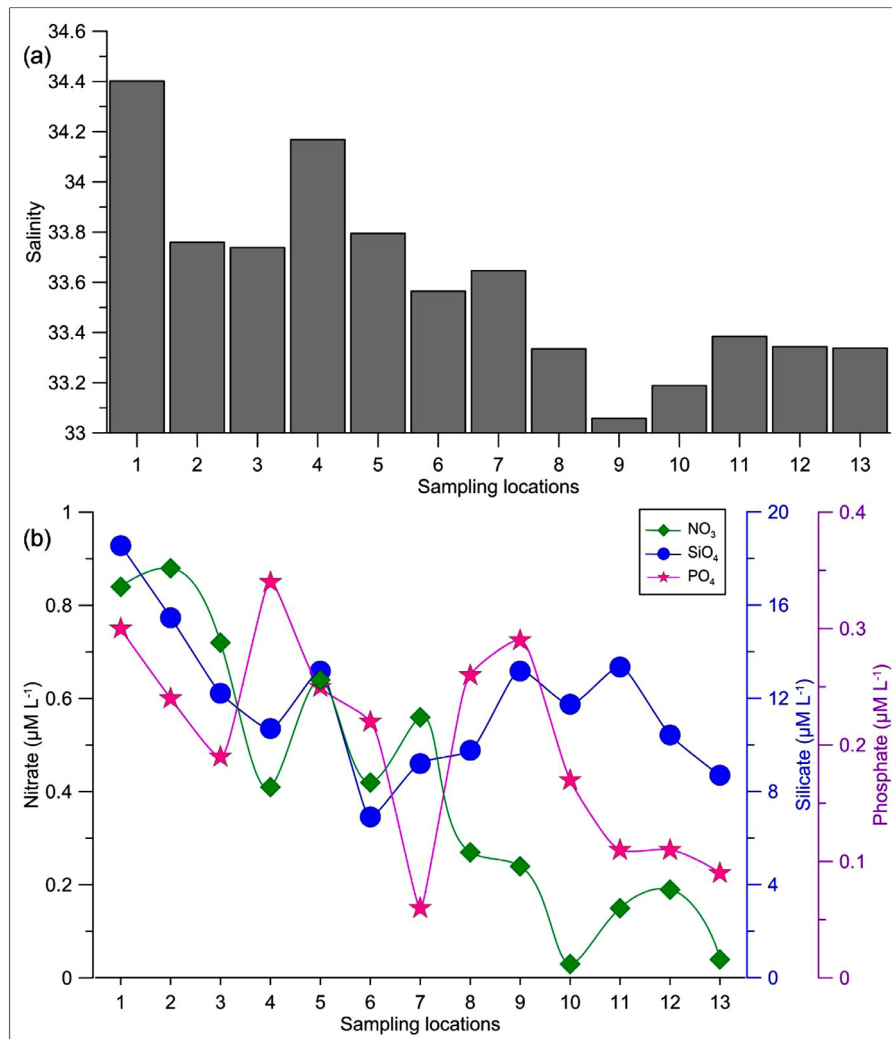
Figure 6 (a) The sea surface salinity of sampling locations indicating high salinity along with the coastal locations (1—7) and relatively low salinity in warm-core eddy locations (8—13). In panel (b), the distribution of major nutrients in the sampling locations is shown.

phytoplankton were higher in the locations closer to the continental shelf (av. 227 $\pm$ 143 ind. L^{-1} and av. 0.8 $\pm$ 0.5 μgC L^{-1}, respectively) (Table 1). The abundance and biomass of micro-autotrophs were noticeably low (av. 13 $\pm$ 9 ind. L^{-1}; av. 0.1 $\pm$ 0.04 μgC L^{-1}) in the warm-core eddy locations (Figure 8a; Table 1). However, interestingly, the individual size of micro-phytoplankton was quite different from the total abundance and biomass pattern; shelf (non-eddy) locations had smaller-sized individuals (av. 50,115 $\pm$ 21,578 μm^3 ind.$^{-1}$) as compared to the warm-core and cold-core eddy infested locations (av. 91760 $\pm$ 12902 μm^3 ind.$^{-1}$). The mean diameter of individual plankton varied from 48.8 $\pm$ 29.7 to 79 $\pm$ 57.6 μm and the diameter size was slightly smaller for those found in the shelf waters (Figure 8b). The shape factor (AR) indicated that most of the locations were dominated by cylindrical/needle-shaped phytoplankton (AR=0.15 $\pm$ 0.19; Figure 8c). Irrespective of locations, the contribution of spherical and elliptical phytoplankton was smaller. The abundance and biomass were positively correlated to salinity and nutrients but negative to SST, MSLA and individual biovolume (Figure 10a). The

community analysis of micro-autotrophs showed that the entire sampling region had the presence of the cyanobacterium *Trichodesmium* (av. 76 $\pm$ 13.4%). The abundance of *Trichodesmium* filaments was quite high in boundary locations of the warm-core eddy. Other forms of autotrophs found in the study area were *Rhizosolenia, Thalassiosira, Cerataulina, Ceratium, Thalassionema, Skeletonema* and *Chaetoceros* (Supplementary Table 1).

3.7. Heterotrophic plankton composition, size and shape

Heterotrophic micro-plankton showed relatively more abundance (av. 15 $\pm$ 5 ind. L^{-1}) and biomass (av. 0.3 $\pm$ 0.1 μgC L^{-1}) in the shelf waters, away from the warm-core eddy infested regions. In the warm-core eddy area, their abundance and biomass were low (av. 6 $\pm$ 4 ind. L^{-1} and av. 0.2 $\pm$ 0.2 μg C L^{-1}; Figure 9a). Relatively larger individuals were found in the eddy-infested offshore region (av. 347 $\pm$ 175 $\times$ 10^3 μm^3 ind.$^{-1}$) compared to those found in the shelf region (av. 229 $\pm$ 62 $\times$ 10^3 μm^3 ind.$^{-1}$). Though the

Table 1 The physicochemical and biological parameters recorded in the *in situ* and satellite data collections.

|	1	2	3	4	5	6	7	8	9	10	11	12	13
SST (°C)	29.1	29.8	29.6	29.6	29.4	29.3	29.5	29.7	29.6	29.6	29.6	29.7	29.7
SAL (PSU)	34.4	33.8	33.7	34.2	33.8	33.6	33.6	33.3	33.1	33.2	33.4	33.3	33.3
DEN (kg/m³)	22	21.1	21.1	21.4	21.2	20.9	20.8	20.4	20.2	20.6	20.6	20.6	20.7
MSLA (cm)	3	-1.4	-2.3	7.4	0.1	1	-0.2	-3.3	-0.8	26.6	26.5	14.2	36.3
MLD (m)	15.5	2.5	6	17	3	3.5	9	1.5	1.5	22.5	5	6	5.5
NO$_3$ (μM/L)	0.84	0.88	0.72	0.41	0.64	0.42	0.56	0.27	0.24	0.03	0.15	0.19	0.04
PO$_4$ (μM/L)	0.3	0.24	0.19	0.34	0.25	0.22	0.06	0.26	0.29	0.17	0.11	0.11	0.09
SiO$_4$ (μM/L)	18.6	15.5	12.2	10.7	13.2	6.9	9.2	9.8	13.2	11.8	13.4	10.4	8.7
Chl (mg/m³)	0.89	0.56	0.73	0.13	0.66	0.3	0.19	0.16	0.15	0.13	0.12	0.13	0.11
A.Abundance (ind./L)	496	309	141	217	116	72	238	14	143	6	8	26	11
A.Biomass (μg C/L)	0.70	0.73	0.55	1.29	0.24	0.39	1.70	0.15	0.72	0.04	0.08	0.13	0.07
A.Vol. (× 10³ μm³/ind.)	29.5	37.2	49.0	62.9	24.5	62.8	85.0	106.4	84.7	81.3	110.5	89.2	86.0
H.Abundance (ind./L)	17.20	14.20	18.60	6.60	10.00	16.00	23.00	8.00	16.50	4.40	3.00	4.60	11.80
H.Biomass (μg C/L)	0.36	0.33	0.30	0.12	0.11	0.19	0.38	0.08	0.21	0.10	0.05	0.07	0.55
H.Vol. (× 10³ μm³/ind.)	318	296	199	226	138	190	236	152	189	316	272	201	601

mean diameter did not varied much among the sampling locations (Figure 9b), the heterotrophic plankton biovolume was slightly higher in the warm-core eddy locations. Most of the organisms showed elliptical to spherical shape bodies (AR=0.64 ± 0.2; Figure 9c). *Tintinnopsis, Protoperidinium,* copepod nauplii, Radiolarians, *Podolampus* and *Stelladinium* were found to be dominant in the study region (Supplementary Table 1). Heterotrophs showed a positive relation to the abundance and biomass of autotrophs (Figure 10a).

4. Discussion

During the Pre-Southwest Monsoon, the BoB is characterised by very weak winds, high solar radiation and warm sea surface, which cause thermally stratified conditions with low plankton production (Gomes et al., 2000; Jyothibabu et al., 2008; Madhu et al., 2006). The BoB is frequented with mesoscale eddies/gyres (both warm-core and cold-core), which have been subjects of unprecedented research interest in the recent decades (Jyothibabu et al., 2015; Murty et al., 2000; Prasanna Kumar et al., 2002; Sarma et al., 2020; Vinayachandran et al., 2009). The mesoscale features can increase plankton production by introducing subsurface nutrients to the surface, as in the case

of cold-core/cyclonic eddies, or it can decrease the biological production by the sinking of warm, nutrient-depleted surface waters as in the case of warm-core/anticyclonic eddies (Jyothibabu et al., 2015; Prasanna Kumar et al., 2002; Vinayachandran et al., 2009). The *in situ* and satellite datasets of SST for the present study period showed a clear warm pool of water ($> 29°C$) centred in the study area. The warm pool stayed for a prolonged period exceeding a one month duration. The geostrophic currents and MSLA of the region showed anticyclonic circulation with positive MSLA, clearly indicating the occurrence of mesoscale warm-core eddy/gyre in the study region. It is clear in the present analysis that SST and MSLA were closely coinciding in the sampling domain, evidencing the convergence of warmer, low salinity and nutrient-impoverished surface water at the centre of the mesoscale warm-core eddy.

Mesoscale ocean surface features in the open seas could be demarcated using satellite data to understand the associated biogeochemical processes (Sarma et al., 2018; Vinayachandran et al., 2009). As shown by Vinayachandran et al. (2009), a mean sea level ≥ 10 cm along with the circulation currents can be considered as the minimum criteria to demarcate the occurrence of mesoscale eddies. In the present study, ≥ 20 cm area was considered to understand the direct impact of the warm-core eddy. Studies showed that most of the eddies in the BoB
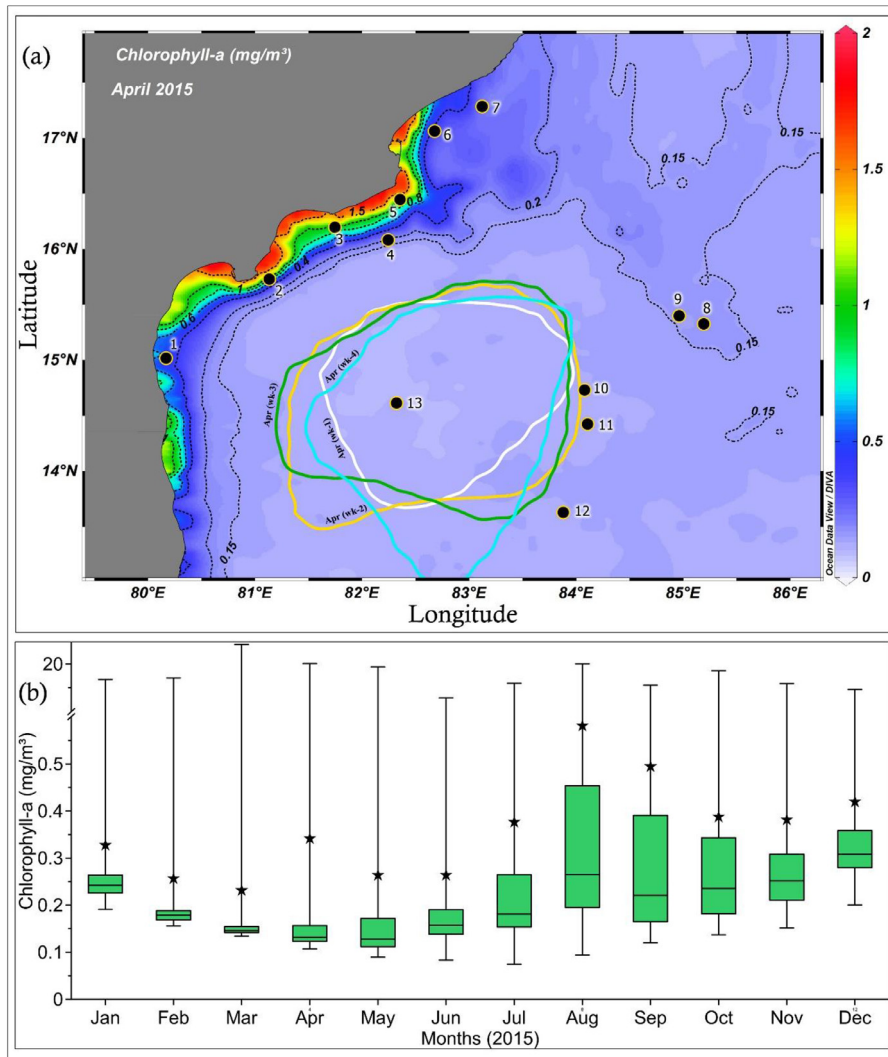
Figure 7 (a) The spatial distribution of chlorophyll-*a* in the sampling domain overlaid with contours of strong warm-core eddy infested area (MSL + 25 cm; continuous lines) and the dotted lines represent chlorophyll-*a* contours. The chlorophyll-*a* values were truncated to 2 mg to remove outliers in the coastal region and to highlight the negative impact of the warm-core eddy. In panel (b) the monthly distribution of surface chlorophyll-*a* in the sampling region and the mean chlorophyll-*a* values are marked with star symbols.

were formed in the eastern/northeastern BoB and moved towards the western/southwestern BoB (Chen et al., 2012; Cheng et al., 2018). Though many eddies were generated in the eastern BoB, its western part also showed a moderate number of eddy formations (Chen et al., 2012). The present study showed the dominant role of EICC in the formation and strengthening of the warm-core eddy along the east coast of India created by spin-up and pinched off from the main path of EICC (Durand et al., 2009; Rennie et al., 2007; Sanilkumar et al., 1997). The EICC was stronger (velocity > 0.7 m s^{-1}) and flowing northward along the coast during the sampling period, it was deflected towards the offshore and in the opposite direction due to curved coastline geometry around the Krishna-Godavari delta in the sampling domain of the Indian sub-continent (~16°N) (Figure 10b). The weekly analysis of mesoscale eddies showed the dominance of larger, stronger and prolonged warm-core eddy persisting in the sampling domain with an area of ~93,580 km^2

and diameter ~345 km, over a month. The deflected water current fed such a large anticyclonic eddy with warmer, nutrient-depleted water mass, which leads to the extremely low chlorophyll-*a* production in the surface waters. The weekly MSLA contours (25 cm) were overlaid on the chlorophyll-*a* image and demarcated the close linkage between the warm-core eddy and low chlorophyll-*a* concentration regions.

The present study showed low chlorophyll-*a* in the surface waters of the warm core eddy region, which can be attributed to the convergence of oligotrophic surface warm waters. On the other hand, the cold-core eddy regions have slightly higher chlorophyll-*a*, but it was not significantly reflected in the abundance and biomass of microplankton. A possible reason for it could be the weaker impact of the cold-core eddy in the study region in bringing up nutrients to the surface layers due to the strong surface layer stratification (Gauns et al., 2005; Gopalakrishna et al., 2002;
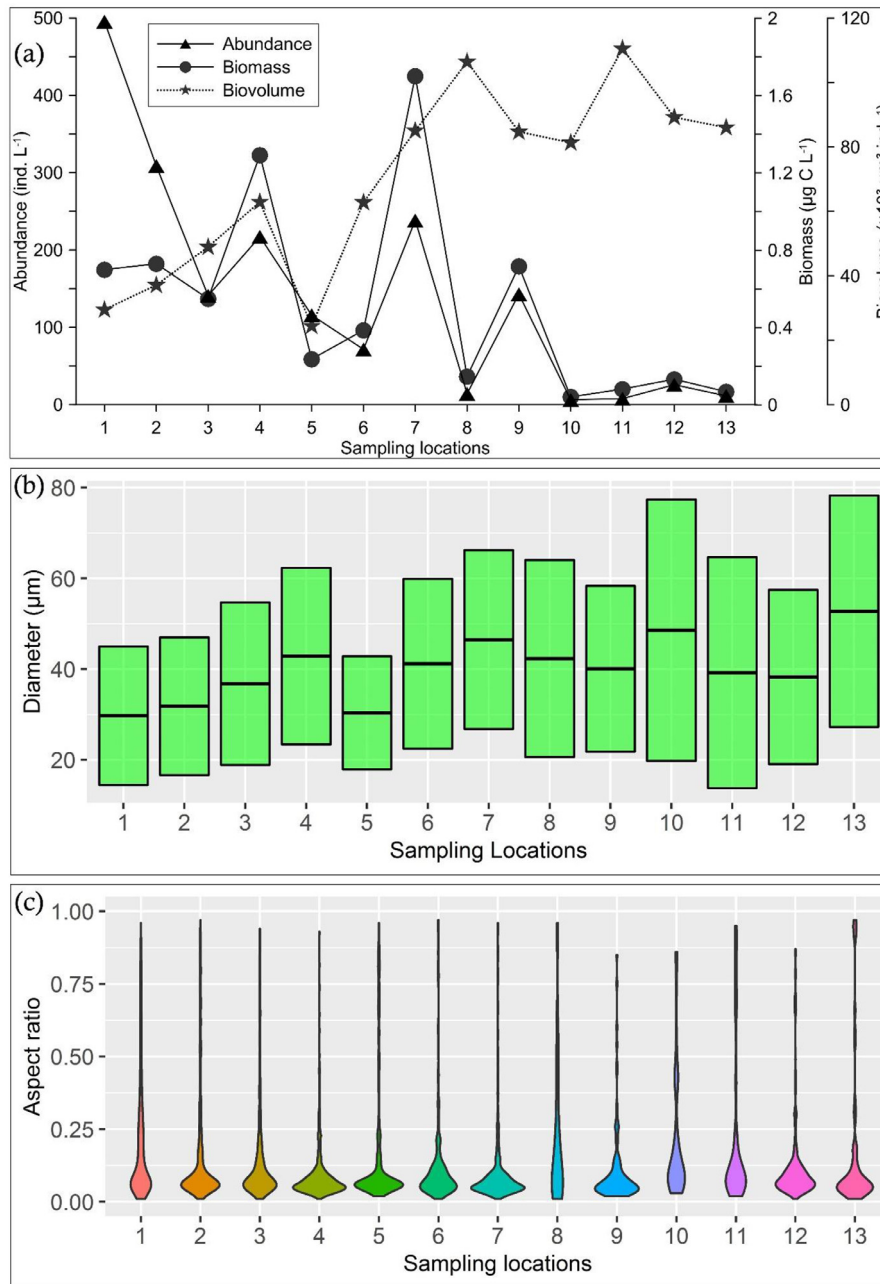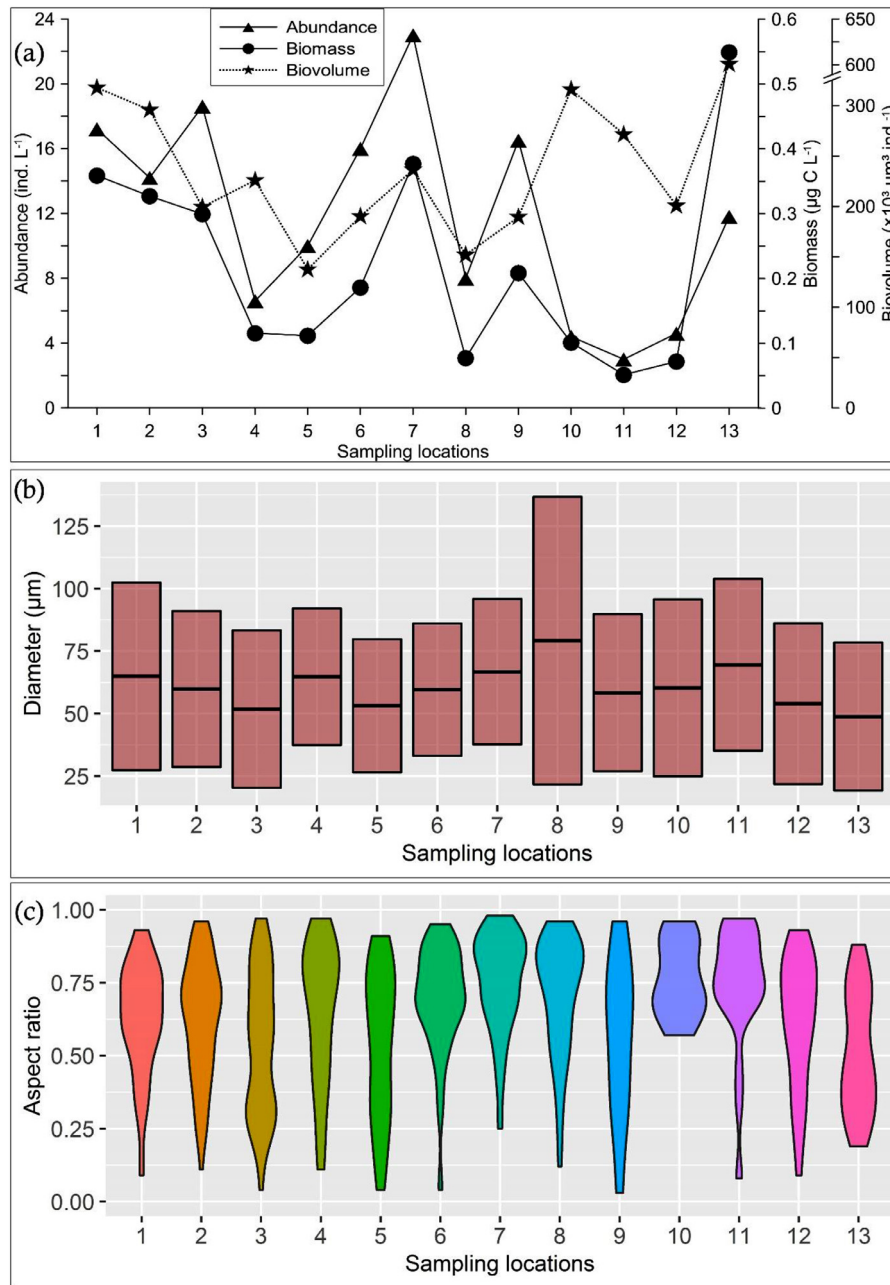
Figure 8 The FlowCAM derived data showing the autotrophic plankton distribution in the sampling locations, (a) abundance, biomass and biovolume, (b) mean diameter of individuals (±SD), and (c) aspect ratio showing the shape of the autotrophs, the area represents the relative frequency of microautotrophs.

Jyothibbau et al., 2008). The high in abundance chlorophyll-*a* patches found north of 16°N along the coast were due to the presence of a cold-core eddy in the shelf region, whereas the extended high chlorophyll-*a* patches towards the open sea could be caused by the combined effect of the cold-core eddy and the EICC that advects water from the shelf and cold-core eddy.

Usually, the highest eddy kinetic energy reported in the western BoB during Pre-Southwest Monsoon is due to instability in the flow of EICC (Chen et al., 2012, 2018). The present study showed a high velocity of geostrophic currents along the boundaries of warm-core eddies. Also, the

height of the core of warm-core eddy varied from 34.7 cm to 38.6 cm with the more energetic flow (> 0.7 m s^{-1}) around which indicates strong convergence, it ultimately leads to the deep sinking of the surface water (Sarma et al., 2018). The strong convergence and associated down-welling help to ventilate the oxygen to deep seas (> 100 m), where oxygen is in demand for bacterial decomposition of organic matter (Mahadevan, 2014; Sarma et al., 2018). A deep and shallow chlorophyll-*a* maxima layers, typical of the warm-core and cold-core eddies, respectively, were also found in this study (Supplementary Figure 1). Earlier studies have shown that strong stratification in the BoB due to the higher

Figure 9 FlowCAM data showing the heterotrophic plankton distribution in each location (a) abundance, biomass and biovolume, (b) mean diameter of individuals (± SD), and (c) aspect ratio to represent the shape of heterotrophs, the area represents the relative frequency of microheterotrophs.

influx of freshwater and weaker mixing, restricts the convergence effect of the cold-core eddies below 20 m in the subsurface (Babu et al., 1991; Gopalakrishna et al., 2002; Gordon et al., 2017; Prasanna Kumar et al., 2007). Even the coastal upwelling is very much limited to the northern BoB due to the strong capping effect of low saline water (Shetye et al., 1991). In such a region during Pre-Southwest Monsoon (March—May), when the solar heating is highest keeping the water column thermally stratified, the warm-core eddies play a significant role in injecting warmer and less-dense surface water into deep seas due to the anticyclonic circulations. Focused *in situ* studies along with nu-

merical modelling are required to comprehend the energy utilization and mixing depths of warm- and cold-core eddies in stratified water columns and their implications on biogeochemical processes.

Along with the physical structure of the water mass, the availability of macronutrients such as nitrate, phosphate and silicate also determines the phytoplankton abundance, biomass, size and community structure in aquatic systems (Sarma et al., 2020; Tilman et al., 1982; Turner et al., 1998; Zhou et al., 2008). The availability of the seasonal highest solar radiation and the significantly low concentration of nutrients at the surface water caused the lowest seasonal
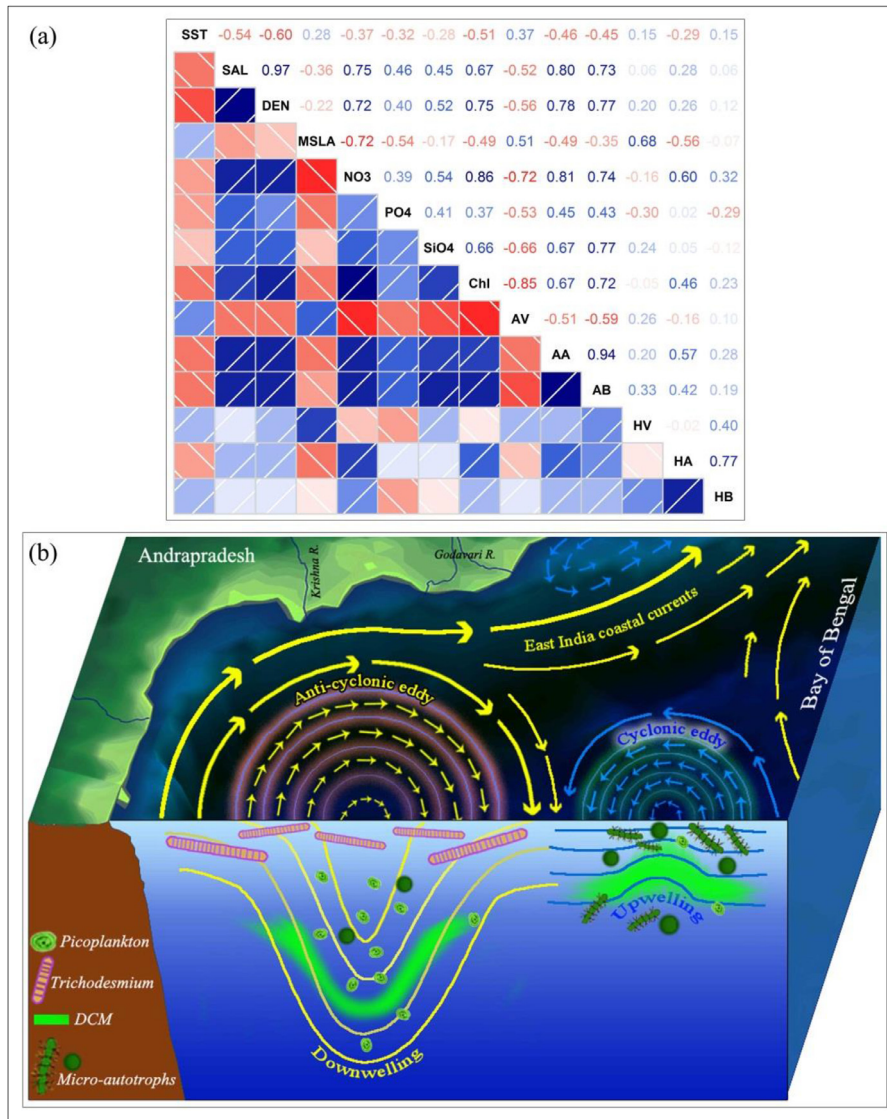
Figure 10 (a) Correlogram shows the relationship between the physicochemical and biological variables in the study domain. In the lower-left diagonal, red colour shade with downslope lines inside represents negative and blue shade with upslope lines represents positive correlation. The correlation coefficients presented in upper right diagonal with red (negative) and blue (positive) colours. Abbreviations: SST: Sea surface temperature; SAL: salinity; DEN: density; MSLA: mean sea level anomaly; NO3: nitrate; PO4: phosphate; SiO4: silicate; Chl: Chlorophyll-*a*; AV: biovolume of autotrophs; AA: the abundance of autotrophs; AB: biomass of autotrophs; HV: biovolume of heterotrophs; HA: the abundance of heterotrophs; and HB: biomass of heterotrophs. Panel (b) presents a conceptual diagram of the eddy features in the Bay of Bengal. The extent of anti-cyclonic eddy (convergence; yellow arrows and contours) is stronger in the Bay of Bengal as compared to the cyclonic eddy (divergence; blue arrows and contours) in vertical penetration. The contour lines in the vertical water column can be considered as water temperature distribution. The depth of Deep Chlorophyll Maxima (DCM) layer shifted vertically as response to the type of eddies depicted.

abundance and biomass of autotrophs in the present study domain. On the other hand, the locations in the shelf waters beyond the warm-core eddy had relatively high abundance and biomass of micro-autotrophs due to moderately high concentrations of nutrients. The microplankton samples analysed through FlowCAM showed the presence of smaller-sized autotrophs in locations in the shelf waters outside the warm-core eddy and relatively large individuals in the mesoscale warm-core eddy region. The Pre-Southwest Monsoon season favours the blooming of cyanobacterium *Trichodesmium* sp., and warm-core eddies increase the

chances of formation of such blooms (Jyothibabu et al., 2017). The larger sized micro-autotrophs recorded in the FlowCAM analysis were *Trichodesmium* filaments. However, the autotrophs found in the high-light water column (near-surface) showed a low concentration of light-harvesting pigments and a comparatively high quantity of photo-protective pigments (Jyothibabu et al., 2018). This also could be one of the reasons for low chlorophyll-*a* in the surface waters and deepened chlorophyll maxima layers in both warm- and cold-core locations. The FlowCAM data evidenced the predominant occurrence of cylindrical/needle

shape phytoplankton in the all sampling locations, which indicates the oligotrophic situation where the high-surface area (to volume) of needle shape phytoplankton used to assimilate low concentration of nutrients more efficiently as compared to spherical phytoplankton (lesser surface-area to volume).

It is well known that numerous long-living mesoscale ocean features occur in the BoB throughout the year (Chen et al., 2012; Dandapath and Chakraborty, 2016). Our recent study based on longtime satellite data analyses revealed that a large area in the BoB is occupied by warm-core as compared to cold-core features throughout the year which leads to oligotrophic and low productive BoB (Jyothibabu et al., 2021). As stated in the previous section, Jyothibabu et al. (2017) showed that the warm-core eddies in the northern Indian Ocean are inducers of *Trichodesmium* blooms. It is showed that the *Trichodesmium* stock sinks along with the converged water mass (warm-core eddy) to the deep where it gets an optimum temperature, light and nutrients to proliferate (Mahadevan et al., 2012). During the growth period, *Trichodesmium* filaments attach and move to the surface by buoyancy (Capone et al., 1997). The individual filaments or bundles tend to migrate to the sea surface along the eddy boundaries where the eddy suction is neutralized by the *in situ* water mass (Mahadevan et al., 2012). In the present study, we excluded longer filaments and colonies (tufts and puffs), which are larger than 300 μm in diameter, to avoid clogging in the flow cell of the FlowCAM. However, FlowCAM data evidenced the relatively high occurrence of *Trichodesmium* filaments in the warm-core eddy locations and diatoms in the non-warm-core eddy locations. Though *Trichodesmium* sp. was abundant in the surface waters, low chlorophyll-*a* showed in satellite as well as *in situ* analysis could be caused by the impact of the highest light at the surface, as stated above, which could significantly decrease/deactivate light-harvesting pigments (Jyothibabu et al., 2018).

The abundance of micro-heterotrophs depends on the environmental conditions and the occurrence of pico and nanoplankton, which are their most preferred food items (Bernard and Rassoulzadegan, 1990; Rassoulzadegan et al., 1988). Due to extreme oligotrophy and the warmer water mass in the warm-core eddy, the availability of such smaller plankton could be lesser than in the coastal and nutrient-rich waters. The lowest organic matter production in such an oligotrophic environment could also reduce the bacterial production, which has a vital role in the microbial pathway of energy transfer to micro-heterotrophs directly and through heterotrophic nanoflagellates (Bernard and Rassoulzadegan, 1990; Jurgens et al., 1996). Focused studies with high-resolution sampling are required to comprehend the distribution and response of micro-heterotrophs to the warm-core eddies as reported by Jagadeesan et al. (2019) in a cold-core eddy in the western BoB for mesozooplankton.

Based on the understanding from present and previous studies, we have made a schematic picture of the western BoB (Figure 10b), which depicts that the deflection of EICC generates mesoscale eddies and the deep chlorophyll layers are significantly pushed-down in the converging warm-core eddy (clock-wise/anticyclonic circulation) and lifted up in the diverging cold-core eddy (counter clock-wise/cyclonic circulation). Also, the warm-core eddy creates an olig-

otrophic condition that supports abundant *Trichodesmium* filaments in the surface waters (Jyothibabu et al., 2017) and pico-autotrophs in the entire water column (Sarma et al., 2020). Conversely, the cold-core eddy supports abundant micro-autotrophs by bringing-up nutrients from the deep sea (Sarma et al., 2020). The size-fractionated primary production measurements in the warm-core, cold-core and no-eddy regions in the BoB during the onset of Southwest Monsoon verified that the micro-autotrophic plankton production was ~2.7 times higher in the cold-core eddy compared to the warm-core eddy (Sarma et al., 2020). Studies have reported the frequent occurrence of *Trichodesmium* blooms in the surface waters of the BoB (Hegde et al., 2008; Jyothibabu et al., 2003, 2014). It is fairly known now that warm-core eddies in the northern Indian ocean provide conducive environmental conditions for the formation of *Trichodesmium* blooms (Jyothibabu et al., 2017). Given this fact, the present study showed that larger micro-autotrophs in the warm-core eddy region were mainly contributed by the *Trichodesmium*, a characteristic feature of extreme oligotrophic warm-core eddies. We propose that the traditional belief that phytoplankton size decreases significantly in oligotrophy (Agawin et al., 2000; Raven, 1986), may not be so much foolproof in warm-core eddy regions of the northern Indian ocean.

5. Conclusion

The present study utilized *in situ* as well as various satellite datasets to understand the impacts of mesoscale warm-core eddies on chlorophyll-*a* and micro-plankton size structure in the western BoB. The warm-core mesoscale eddy persisted during the Pre-Southwest Monsoon period in the sampling region with an area of ~93,580 km^2 and diameter ~345 km ($\geq$ 20 cm MSLA), strongly reducing the surface chlorophyll-*a* (av. 0.1 $\pm$ 0.01 mg m^{-3}). The satellite-based MSLA and chlorophyll-*a* analysis showed a strong negative correlation between each other and the prolonged existence of warm-core eddies in a large area of the study domain. The warmer and nutrient-depleted water mass in the warm-core eddy facilitated the high abundance of the cyanobacteria species *Trichodesmium* instead of the usual micro-autotrophs such as diatoms and dinoflagellates. The mesoscale warm-core eddy occupied waters showed > 6 fold lesser abundance and biomass of micro-autotrophs as compared to the non-eddy regions. On the other hand, a high abundance of smaller-sized micro-autotrophs was found outside the warm-core eddy. These features present the view that the usual notion that the intensification of oligotrophy favours the decrease in size of autotrophs in marine systems may not be fully true in warm-core eddy regions in the northern Indian ocean infested with high *Trichodesmium* filaments. The low production in the warm-core eddy is also reflected by lower abundance and biomass of micro-heterotrophs as compared to the coastal waters.

Declaration of Competing Interest

The authors declare that they have no known competing financial interests or personal relationships that could have appeared to influence the work reported in this paper.

Supplementary materials

Supplementary material associated with this article can be found, in the online version, at https://doi.org/10.1016/j.oceano.2021.02.003.

References

Agawin, N.S.R., Duarte, C.M., Agusti, S., 2000. Nutrient and temperature control of the contribution of picoplankton to phytoplankton biomass and production. Limnol. Oceanogr. 45, 591−600. https://doi.org/10.4319/lo.2000.45.3.0591

Alvarez, E., Lopez-Urrutia, A., Nogueira, E., 2012. Improvement of plankton biovolume estimates derived from image-based automatic sampling devices: application to FlowCAM. J. Plankton Res. 34, 454−469. https://doi.org/10.1093/plankt/fbs017

Azam, F., Fenchel, T., Field, J.G., Gray, J.S., Meyer-Reil, L.A., Thingstad, F., 1983. The ecological role of water-column microbes in the sea. Mar. Ecol. Prog. Ser. 10, 257−263. https://doi.org/10.3354/meps010257

Babu, M.T., Prasanna Kumar, S., Rao, D.P., 1991. A subsurface cyclonic eddy in the Bay of Bengal. J. Mar. Res. 49, 403−410. https://doi.org/10.1357/002224091784995846

Bernard, C., Rassoulzadegan, F., 1990. Bacteria or microflagellates as a major food source for marine ciliates: possible implications for the microzooplankton. Mar. Ecol. Prog. Ser. Oldendorf 64, 147−155. https://www.jstor.org/stable/24844600

Capone, D.G., Zehr, J.P., Paerl, H.W., Bergman, B., Carpenter, E.J., 1997. Trichodesmium, a globally significant marine cyanobacterium. Science 276, 1221−1229. https://doi.org/10.1126/science.276.5316.1221

Chaigneau, A., Gizolme, A., Grados, C., 2008. Mesoscale eddies off Peru in altimeter records: Identification algorithms and eddy spatio-temporal patterns. Prog. Oceanogr. 79, 106−119. https://doi.org/10.1016/j.pocean.2008.10.013

Chassot, E., Bonhommeau, S., Dulvy, N.K., Melin, F., Watson, R., Gascuel, D., Le Pape, O., 2010. Global marine primary production constrains fisheries catches. Ecol. Lett. 13, 495−505. https://doi.org/10.1111/j.1461-0248.2010.01443.x

Chelton, D.B., Gaube, P., Schlax, M.G., Early, J.J., Samelson, R.M., 2011. The influence of nonlinear mesoscale eddies on near-surface oceanic chlorophyll. Science 334, 328−332. https://doi.org/10.1126/science.1208897

Chen, G., Li, Y., Xie, Q., Wang, D., 2018. Origins of eddy kinetic energy in the Bay of Bengal. J. Geophys. Res. Oceans 123, 2097−2115. https://doi.org/10.1002/2017JC013455

Chen, G., Wang, D., Hou, Y., 2012. The features and interannual variability mechanism of mesoscale eddies in the Bay of Bengal. Cont. Shelf Res. 47, 178−185. https://doi.org/10.1016/j.csr.2012.07.011

Cheng, X., McCreary, J.P., Qiu, B., Qi, Y., Du, Y., Chen, X., 2018. Dynamics of eddy generation in the central Bay of Bengal. J. Geophys. Res. Oceans 123, 6861−6875. https://doi.org/10.1029/2018JC014100

Dandapat, S., Chakraborty, A., 2016. Mesoscale eddies in the Western Bay of Bengal as observed from satellite altimetry in 1993-2014: statistical characteristics, variability and three-dimensional properties. IEEE J. Sel. Top. Appl. Earth Obs. Remote Sens. 9, 5044−5054. https://doi.org/10.1109/JSTARS.2016.2585179

Durand, F., Shankar, D., Birol, F., Shenoi, S.S.C., 2009. Spatiotemporal structure of the East India Coastal Current from satellite altimetry. J. Geophys. Res. Oceans 114. https://doi.org/10.1029/2008JC004807

Friendly, M., 2002. Corrgrams: Exploratory displays for correlation matrices. Am. Stat. 56, 316−324. https://doi.org/10.1198/000313002533

Garrison, D.L., Gowing, M.M., Hughes, M.P., Campbell, L., Caron, D.A., Dennett, M.R., Shalapyonok, A., Olson, R.J., Landry, M.R., Brown, S.L., 2000. Microbial food web structure in the Arabian Sea: a US JGOFS study. Deep Sea Res. Part II Top. Stud. Oceanogr. 47, 1387−1422. https://doi.org/10.1016/S0967-0645(99)00148-4

Gauns, M., Madhupratap, M., Ramaiah, N., Jyothibabu, R., Fernandes, V., Paul, J.T., Kumar, S.P., 2005. Comparative accounts of biological productivity characteristics and estimates of carbon fluxes in the Arabian Sea and the Bay of Bengal. Deep Sea Res. Pt. II Top. Stud. Oceanogr. 52, 2003−2017. https://doi.org/10.1016/j.dsr2.2005.05.009

Gomes, H.R., Goes, J.I., Saino, T., 2000. Influence of physical processes and freshwater discharge on the seasonality of phytoplankton regime in the Bay of Bengal. Cont. Shelf Res. 20, 313−330. https://doi.org/10.1016/S0278-4343(99)00072-2

Gopalakrishna, V.V., Murty, V.S.N., Sengupta, D., Shenoy, S., Araligidad, N., 2002. Upper ocean stratification and circulation in the northern Bay of Bengal during southwest monsoon of 1991. Cont. Shelf Res. 22, 791−802. https://doi.org/10.1016/S0278-4343(01)00084-X

Gordon, A.L., Shroyer, E., Murty, V.S.N., 2017. An Intrathermocline Eddy and a tropical cyclone in the Bay of Bengal. Sci. Rep. 7, 46218. https://doi.org/10.1038/srep46218

Grasshoff, K., Ehrhardt, M., Kremling, K., 1983. Methods of Seawater Analysis. Verlag Chemie, Weinheim, 89−224.

Harrison, P.J., Zingone, A., Mickelson, M.J., Lehtinen, S., Ramaiah, N., Kraberg, A.C., Sun, J., McQuatters-Gollop, A., Jakobsen, H.H., 2015. Cell volumes of marine phytoplankton from globally distributed coastal data sets. Estuar. Coast. Shelf Sci. 162, 130−142. https://doi.org/10.1016/j.ecss.2015.05.026

Hegde, S., Anil, A.C., Patil, J.S., Mitbavkar, S., Krishnamurthy, V., Gopalakrishna, V.V., 2008. Influence of environmental settings on the prevalence of Trichodesmium spp. in the Bay of Bengal. Mar. Ecol. Prog. Ser. 356, 93−101. https://doi.org/10.3354/meps07259

Jagadeesan, L., Kumar, G.S., Rao, D.N., Srinivas, T.N.R., 2019. Role of eddies in structuring the mesozooplankton composition in coastal waters of the western Bay of Bengal. Ecol. Indicators 105, 137−155. https://doi.org/10.1016/j.ecolind.2019.05.068

Jurgens, K., Wickham, S.A., Rothhaupt, K.O., Santer, B., 1996. Feeding rates of macro-and microzooplankton on heterotrophic nanoflagellates. Limnol. Oceanogr. 41, 1833−1839. https://doi.org/10.4319/lo.1996.41.8.1833

Jyothibabu, R., Arunpandi, N., Jagadeesan, L., Karnan, C., Lallu, K.R., Vinayachandran, P.N., 2018. Response of phytoplankton to heavy cloud cover and turbidity in the northern Bay of. Bengal. Sci. Rep. 8, 1−15. https://doi.org/10.1038/s41598-018-29586-1

Jyothibabu, R., Karnan, C., Jagadeesan, L., Arunpandi, N., Pandiarajan, R.S., Muraleedharan, K.R., Balachandran, K.K., 2017. Trichodesmium blooms and warm-core ocean surface features in the Arabian Sea and the Bay of Bengal. Mar. Pollut. Bull.

121, 201—215. https://doi.org/10.1016/j.marpolbul.2017.06.002

Jyothibabu, R., Madhu, N.V., Maheswaran, P.A., Jayalakshmy, K.V., Nair, K.K.C., Achuthankutty, C.T., 2008. Seasonal variation of microzooplankton (20-200μm) and its possible implications on the vertical carbon flux in the western Bay of Bengal. Cont. Shelf Res. 28, 737—755. https://doi.org/10.1016/j.csr.2007.12.011

Jyothibabu, R., Madhu, N.V., Murukesh, N., Haridas, P., Nair, K.K.C., Venugopal, P., 2003. Intense blooms of Trichodesmium erythraeum (Cyanophyta) in the open waters along east coast of India. Indian J. Mar. Sci. 32, 165—167. http://hdl.handle.net/123456789/4262

Jyothibabu, R., Vinayachandran, P.N., Madhu, N.V., Robin, R.S., Karnan, C., Jagadeesan, L., Anjusha, A., 2015. Phytoplankton size structure in the southern Bay of Bengal modified by the Summer Monsoon Current and associated eddies: Implications on the vertical biogenic flux. J. Mar. Syst. 143, 98—119. https://doi.org/10.1016/j.jmarsys.2014.10.018

Jyothibabu, R., Win, N.N., Shenoy, D.M., Swe, U.T., Pratik, M., Thwin, S., Jagadeesan, L., 2014. Interplay of diverse environmental settings and their influence on the plankton community off Myanmar during the Spring Intermonsoon. J. Mar. Syst. 139, 446—459. https://doi.org/10.1016/j.jmarsys.2014.08.003

Jyothibabu, R., Karnan, C., Arunpandi, N., Krishnan, S.S., Balachandran, K.K., Sahu, K.C., 2021. Significantly dominant warm-core eddies: An ecological indicator of the basin-scale low biological production in the Bay of. Bengal. Ecol. Indicators 121, 107016. https://doi.org/10.1016/j.ecolind.2020.107016

Karnan, C., Jyothibabu, R., Arunpandi, N., Jagadeesan, L., Muraleedharan, K.R., Pratihari, A.K., Balachandran, K.K., Naqvi, S.W.A., 2017. Discriminating the biophysical impacts of coastal upwelling and mud banks along the southwest coast of India. J. Mar. Syst. 172, 24—42. https://doi.org/10.1016/j.jmarsys.2017.02.012

Landry, M.R., Brown, S.L., Campbell, L., Constantinou, J., Liu, H., 1998. Spatial patterns in phytoplankton growth and microzooplankton grazing in the Arabian Sea during monsoon forcing. Deep Sea Res. Pt. II Top. Stud. Oceanogr. 45, 2353—2368. https://doi.org/10.1016/S0967-0645(98)00074-5

Li, C., Du, Y., Liang, F., Yi, J., Lakhan, V.C., 2015. A GIS-based method for depicting the characteristics of mesoscale eddies: a case study in the Northern South China Sea. Can. J. Earth Sci. 52, 746—756. https://doi.org/10.1139/cjes-2014-0177

Madhu, N.V., Jyothibabu, R., Maheswaran, P.A., Gerson, V.J., Gopalakrishnan, T.C., Nair, K.K.C., 2006. Lack of seasonality in phytoplankton standing stock (chlorophyll a) and production in the western Bay of Bengal. Cont. Shelf Res. 26, 1868—1883. https://doi.org/10.1016/j.csr.2006.06.004

Madhupratap, M., Gauns, M., Ramaiah, N., Kumar, S.P., Muraleedharan, P.M., De Sousa, S.N., Sardessai, S., Muraleedharan, U., 2003. Biogeochemistry of the Bay of Bengal: physical, chemical and primary productivity characteristics of the central and western Bay of Bengal during summer monsoon 2001. Deep Sea Res. Pt. II Top. Stud. Oceanogr. 50, 881—896. https://doi.org/10.1016/S0967-0645(02)00611-2

Mahadevan, A., 2014. Ocean science: Eddy effects on biogeochemistry. Nature 506, 168—169. https://doi.org/10.1038/nature13048

Mahadevan, A., D'asaro, E., Lee, C., Perry, M.J., 2012. Eddy-driven stratification initiates North Atlantic spring phytoplankton blooms. Science 337, 54—58. https://science.sciencemag.org/content/337/6090/54

McGillicuddy, D.J., Anderson, L.A., Doney, S.C., Maltrud, M.E., 2003. Eddy-driven sources and sinks of nutrients in the upper ocean: Results from a 0.1 resolution model of the North Atlantic. Glob. Biogeochem. Cy. 17. https://doi.org/10.1029/2002GB001987

McGillicuddy, D.J., Robinson, A.R., Siegel, D.A., Jannasch, H.W., Johnson, R., Dickey, T.D., McNeil, J., Michaels, A.F., Knap, A.H., 1998. Influence of mesoscale eddies on new production in the Sargasso Sea. Nature 394, 263—266. https://doi.org/10.1038/28367

Menden-Deuer, S., Lessard, E.J., 2000. Carbon to volume relationships for dinoflagellates, diatoms, and other protist plankton. Limnol. Oceanogr. 45, 569—579. https://doi.org/10.4319/lo.2000.45.3.0569

Mukhopadhyay, S.K., Biswas, H., De, T.K., Jana, T.K., 2006. Fluxes of nutrients from the tropical River Hooghly at the land-ocean boundary of Sundarbans, NE Coast of Bay of Bengal, India. J. Mar. Syst. 62, 9—21. https://doi.org/10.1016/j.jmarsys.2006.03.004

Murty, V.S.N., Gupta, G.V.M., Sarma, V.V., Rao, B.P., Jyothi, D., Shastri, P.N.M., Supraveena, Y., 2000. Effect of vertical stability and circulation on the depth of the chlorophyll maximum in the Bay of Bengal during May-June, 1996. Deep Sea Res. Pt. I Top. Stud. Oceanogr 47, 859—873. https://doi.org/10.1016/S0967-0637(99)00071-0

Patnaik, K., Maneesha, K., Sadhuram, Y., Prasad, K., Ramana Murty, T.V., Brahmananda Rao, V., 2014. East India Coastal Current induced eddies and their interaction with tropical storms over Bay of Bengal. J. Oper. Oceanogr. 7, 58—68. https://doi.org/10.1080/1755876X.2014.11020153

Patra, P.K., Kumar, M.D., Mahowald, N., Sarma, V., 2007. Atmospheric deposition and surface stratification as controls of contrasting chlorophyll abundance in the North Indian Ocean. J. Geophys. Res. Oceans 112. https://doi.org/10.1029/2006JC003885

Prasanna Kumar, S., Muraleedharan, P.M., Prasad, T.G., Gauns, M., Ramaiah, N., De Souza, S.N., Sardesai, S., Madhupratap, M., 2002. Why is the Bay of Bengal less productive during summer monsoon compared to the Arabian Sea? Geophys. Res. Lett. 29 (24), 88-81—88-84. https://doi.org/10.1029/2002GL016013

Prasanna Kumar, S., Narvekar, J., Nuncio, M., Kumar, A., Ramaiah, N., Sardessai, S., Gauns, M., Fernandes, V., Paul, J., 2010. Is the biological productivity in the Bay of Bengal light limited? Curr. Sci. 98, 1331—1339. https://www.jstor.org/stable/24107511

Prasanna Kumar, S., Nuncio, M., Narvekar, J., Kumar, A., Sardesai, S., De Souza, S.N., Gauns, M., Ramaiah, N., Madhupratap, M., 2004. Are eddies nature's trigger to enhance biological productivity in the Bay of Bengal? Geophys. Res. Lett. 31, 1—5. https://doi.org/10.1029/2003GL019274

Prasanna Kumar, S., Nuncio, M., Ramaiah, N., Sardesai, S., Narvekar, J., Fernandes, V., Paul, J.T., 2007. Eddy-mediated biological productivity in the Bay of Bengal during fall and spring intermonsoons. Deep Sea Res. Pt. I Top. Stud. Oceanogr. 54, 1619—1640. https://doi.org/10.1016/j.dsr.2007.06.002

Rassoulzadegan, F., Laval-Peuto, M., Sheldon, R.W., 1988. Partitioning of the food ration of marine ciliates between pico-and nanoplankton. Hydrobiologia 159, 75—88. https://doi.org/10.1007/BF00007369

Raven, J.A., 1986. Physiological consequences of extremely small size for autotrophic organisms in the sea. Photosynthetic Picoplankton 214, 1—70.

Rennie, S.J., Pattiaratchi, C.P., McCauley, R.D., 2007. Eddy formation through the interaction between the Leeuwin Current, Leeuwin Undercurrent and topography. Deep Sea Res. Pt. II Top. Stud. Oceanogr. 54, 818—836. https://doi.org/10.1016/j.dsr2.2007.02.005

Sanilkumar, K.V., Kuruvilla, T.V., Jogendranath, D., Rao, R.R., 1997. Observations of the Western Boundary Current of the Bay of Bengal from a hydrographic survey during March 1993. Deep Sea Res. Pt. I Top. Stud. Oceanogr 44, 135—145. https://doi.org/10.1016/S0967-0637(96)00036-2

Sarma, V., Chopra, M., Rao, D.N., Priya, M.M.R., Rajula, G.R., Lakshmi, D.S.R., Rao, V.D., 2020. Role of eddies on controlling total and size-fractionated primary production in the Bay of Bengal. Cont. Shelf Res. 204, 104186. https://doi.org/10.1016/j.csr.2020.104186

Sarma, V., Jagadeesan, L., Dalabehera, H.B., Rao, D.N., Kumar, G.S., Durgadevi, D.S., Yadav, K., Behera, S., Priya, M.M.R., 2018. Role of eddies on intensity of oxygen minimum zone in the Bay of Bengal. Cont. Shelf Res. 168, 48—53. https://doi.org/10.1016/j.csr.2018.09.008

Shankar, D., McCreary, J.P., Han, W., Shetye, S.R., 1996. Dynamics of the East India Coastal Current: 1. Analytic solutions forced by interior Ekman pumping and local alongshore winds. J. Geophys. Res. Oceans 101, 13975—13991. https://doi.org/10.1029/96JC00559

Shenoi, S.S.C., Shankar, D., Shetye, S.R., 2002. Differences in heat budgets of the near-surface Arabian Sea and Bay of Bengal: Implications for the summer monsoon. J. Geophys. Res. Oceans 107, 5.1—5.14. https://doi.org/10.1029/2000JC000679

Shetye, S.R., Shenoi, S.S.C., Gouveia, A.D., Michael, G.S., Sundar, D., Nampoothiri, G., 1991. Wind-driven coastal upwelling along the western boundary of the Bay of Bengal during the southwest monsoon. Cont. Shelf Res. 11, 1397—1408. https://doi.org/10.1016/0278-4343(91)90042-5

Subramanian, V., 1993. Sediment load of Indian rivers. Curr. Sci. 64, 928—930. https://www.jstor.org/stable/24096213

Tilman, D., Kilham, S.S., Kilham, P., 1982. Phytoplankton community ecology: the role of limiting nutrients. Annu. Rev. Ecol. Syst. 13, 349—372. https://doi.org/10.1146/annurev.es.13.110182.002025

Turner, R.E., Qureshi, N., Rabalais, N.N., Dortch, Q., Justic, D., Shaw, R.F., Cope, J., 1998. Fluctuating silicate: nitrate ratios and coastal plankton food webs. Proc. Natl. Acad. Sci. 95, 13048—13051. https://doi.org/10.1073/pnas.95.22.13048

Verity, P.G., Robertson, C.Y., Tronzo, C.R., Andrews, M.G., Nelson, J.R., Sieracki, M.E., 1992. Relationships between cell volume and the carbon and nitrogen content of marine photosynthetic nanoplankton. Limnol. Oceanogr. 37, 1434—1446. https://doi.org/10.4319/lo.1992.37.7.1434

Vinayachandran, P.N., 2009. Impact of physical processes on chlorophyll distribution in the Bay of Bengal. Geophys. Monogr. Series 185, American Geophysical Union 71—86. https://doi.org/10.1029/2008GM000705

Vinayachandran, P.N., Chauhan, P., Mohan, M., Nayak, S., 2004. Biological response of the sea around Sri Lanka to summer monsoon. Geophys. Res. Lett. 31. https://doi.org/10.1029/2003GL018533

Wong, W.H., Rabalais, N.N., Turner, R.E., 2016. Size-dependent top-down control on phytoplankton growth by microzooplankton in eutrophic lakes. Hydrobiologia 763, 97—108. https://doi.org/10.1007/s10750-015-2365-3

Yentsch, C.S., Phinney, D.A., 1989. A bridge between ocean optics and microbial ecology. Limnol. Oceanogr. 34, 1694—1705. https://doi.org/10.4319/lo.1989.34.8.1694

Zhou, M.-j., Shen, Z.-l., Yu, R.-c., 2008. Responses of a coastal phytoplankton community to increased nutrient input from the Changjiang (Yangtze) River. Cont. Shelf Res. 28, 1483—1489. https://doi.org/10.1016/j.csr.2007.02.009